New Talent: Americas

Guest Editors: John Arnold, Dan Mindiola, Theo Agapie,
Jennifer Love and Mircea Dincă

Published in issue 26, 2012 of *Dalton Transactions*

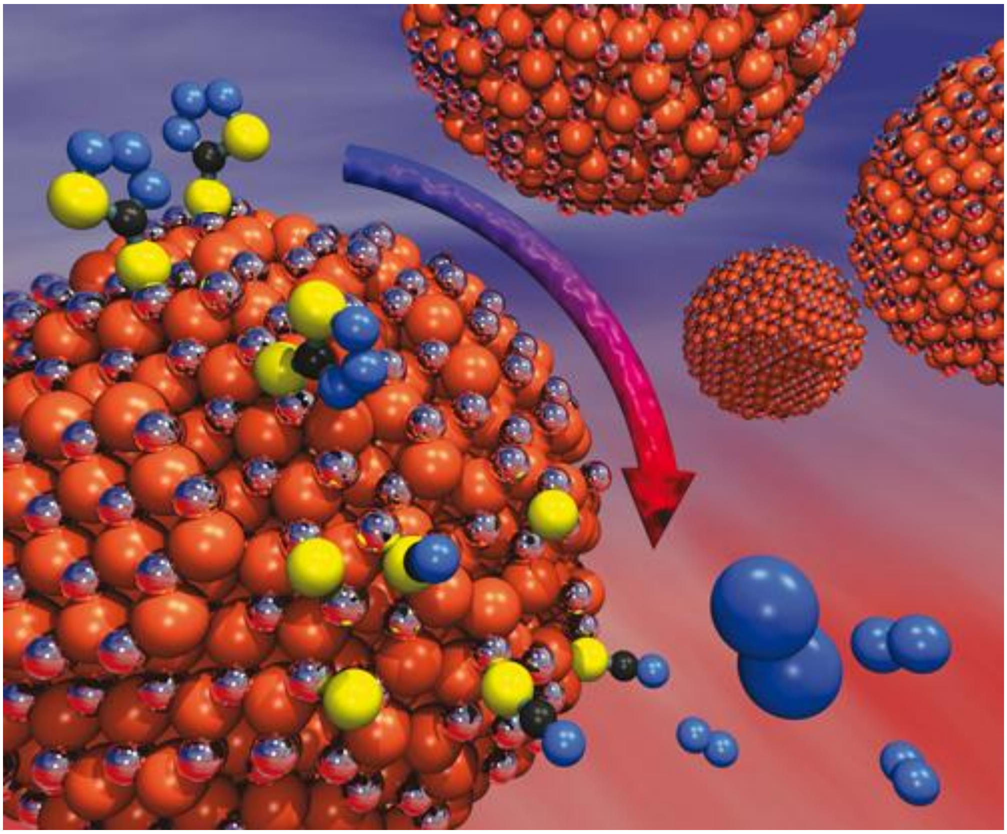

Image reproduced with permission of Richard L. Brutchey

Dalton
Transactions

Dynamic Article Links
View Online

Cite this: *Dalton Trans.*, 2012, **41**, 8031

www.rsc.org/dalton

PAPER

Coordination and structural properties of encumbering 6-mesityl-2-picolinate complexes†

Patrick W. Smith, Curtis E. Moore, Arnold L. Rheingold and Joshua S. Figueroa*

Received 13th March 2012, Accepted 16th April 2012
DOI: 10.1039/c2dt30585b

In an effort to enforce a sterically hindered environment in transition-metal and main-group 2-picolinate complexes, the synthesis of the encumbering derivative 6-mesityl-2-picolinate ($^{\mathrm{Mes}}$pic) is presented. The coordination and structural properties of $^{\mathrm{Mes}}$pic are demonstrated with a range of transition-metal and main-group fragments. The 6-position mesityl group of $^{\mathrm{Mes}}$pic is shown to alter both the primary and secondary coordination spheres of metal centers relative to the ubiquitous and unencumbered parent 2-picolinate anion.

Introduction

The unsubstituted 2-picolinate anion (pyridine-2-carboxylate) is a well-utilized ancillary ligand in coordination chemistry. The longstanding appeal of the 2-picolinate framework is derived from its ability to form a stable, five-membered chelate ring featuring an anionic binding group. In this respect, 2-picolinate is sterically and topologically similar to the ubiquitous neutral 2,2′-bipyridine ligand, yet bears a monoanionic charge. Accordingly, 2-picolinate has been employed in a range of applications, including the synthesis of metal–organic frameworks (MOFs),[1–4] lanthanide chelation/remediation,[5–7] and in the case of the tris-picolinate complex, Cr(pic)$_3$, in a commercial dietary supplement for bioactive chromium ions.[8] In addition, its resistance toward oxidation[9] and strong chelation properties have made 2-picolinate an attractive ligand for the stabilization of transition-metal ions in high formal oxidation states.[10] For this application, Barton's use of iron picolinate complexes for catalytic aerobic alkane oxidation is most notable, as Fe(IV) oxo species are proposed as the critical reactive intermediates.[11]

In addition to this long-standing coordination chemistry, there has been a resurgence of interest in 2-picolinate complexes as reagents in synthesis. This renewed attention has followed Baran's recent utilization of silver(II) 2-picolinate (Ag(pic)$_2$) for the selective, formal C–H bond hydroxylation of guanidinium-containing rings in aqueous media.[12–15] This Ag(II)-mediated oxidation, which is thought to proceed by two discreet one-electron transfer processes,[16] has also been extended to the C–H bond arylation of electron-poor nitrogen heterocycles with aryl boronic acids.[17] Organic oxidation reactions by silver(II) build on the pioneering studies by Lee, who demonstrated that Ag(pic)$_2$ can be employed for the oxidation of aliphatic alcohols to aldehydes[18] and the oxidative decarboxylation of α-amino acids.[19,20] Notably, Ag(pic)$_2$ represents one of the few stable and well-characterized silver(II) complexes.[18–26] This fact further highlights the ability of the 2-picolinate ligand to stabilize transition metals in high formal oxidation-states.

Given the broad utilization of the 2-picolinate anion, it is noteworthy that sterically encumbering variants have not been widely investigated. Substitution at the 6-position specifically, which flanks the metal center in 2-picolinate complexes, has been limited to the 6-methyl[27–33] and 6-ethyl[34,35] derivatives.[36] However, it is reasonable to expect that an encumbering 6-position substituent may help foster hindered or low-coordinate environments for 2-picolinate complexes. Accordingly, in an effort to couple the favorable coordination properties of 2-picolinate with a more sterically encumbered environment, we report here the synthesis of 6-mesityl-2-picolinate ($^{\mathrm{Mes}}$pic; Mes = 2,4,6-$\mathrm{Me_3C_6H_2}$) and detail its coordination ability with transition-metal and main-group fragments. As hoped, the $^{\mathrm{Mes}}$pic ligand can indeed provide a sterically congested coordination environment and can affect the structural chemistry of metal centers to which it is bound. This work is an extension of our related interest in the coordination chemistry of encumbering pyridine ligands that mimic the topological properties of the *m*-terphenyl backbone.[37]

Results and discussion

Scheme 1 shows the synthesis of 6-Mes-2-picolinic acid and several derivatives for use in metallation reactions. Suzuki–Miyaura cross-coupling of methyl 6-bromo-2-picolinate with mesitylboronic acid readily installs a mesityl group on the picolinate framework in good yield (70%). This cross-coupling reaction performs well on scales up to 1.0 g with reasonable loadings of the palladium catalyst-precursor $\mathrm{Pd_2(dba)_3}$ (1.4 mol%; 2.8 mol% Pd; dba = dibenzylideneacetone). Base-

---

Department of Chemistry and Biochemistry, University of California, San Diego, 9500 Gilman Drive, Mail Code 0358, La Jolla, California 92093-0358, USA. E-mail: jsfig@ucsd.edu

† Electronic supplementary information (ESI) available: Crystallographic structure determinations and HRMS data (pdf and cif). CCDC 871423–871426. For ESI and crystallographic data in CIF or other electronic format see DOI: 10.1039/c2dt30585b

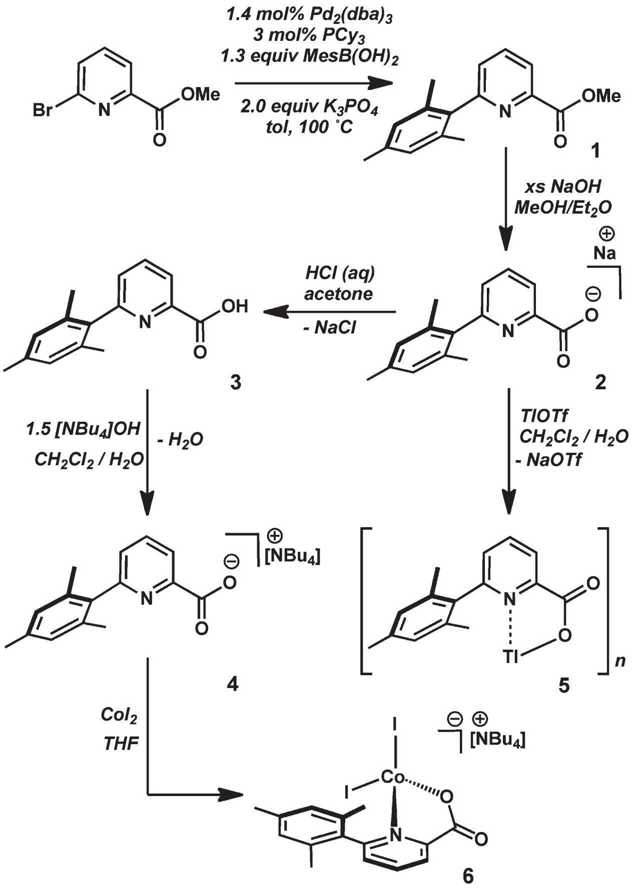

Scheme 1

mediated hydrolysis of the resulting 6-mesityl-2-picolinate methyl ester (**1**) with NaOH provides the sodium salt, Na[^{Mes}pic] (**2**), as a colorless solid. The latter can be obtained in high purity when worked-up under alkaline conditions and is readily converted to the parent acid, ^{Mes}picH (**3**), in a subsequent step by the addition of aqueous HCl. As expected, the encumbering mesityl substituent has a solubilizing effect and allows ^{Mes}picH (**3**) to be dissolved in common ethereal and aromatic solvents. The solid-state IR spectrum (KBr) of ^{Mes}picH features a strong absorption band at 1730 cm^{-1} consistent with the presence of a carbonyl (C=O) unit. The O–H moiety is found as a broad signal centered at 2485 cm^{-1} as is typical for carboxylic acids. Also present in the IR spectrum of ^{Mes}picH are moderately intense bands located at 1610, 1586 and 1447 cm^{-1}, which are indicative of N=C and C=C stretching modes for pyridyl compounds.[38] The ^{1}H NMR spectrum of ^{Mes}picH in dry C_6D_6 solution reveals a broad, downfield signal centered at 10.8 ppm, consistent with the presence of a carboxylic acid proton engaged in either intramolecular (to the pyridine nitrogen atom) or intermolecular hydrogen-bonding interactions.‡ Treatment of ^{Mes}picH (**3**) with tetrabutylammonium hydroxide ([NBu$_4$]OH) in a 1 : 1 CH_2Cl_2–H_2O mixture generates the tetrabutylammonium picolinate salt [NBu$_4$][^{Mes}pic] (**4**), which is insoluble in H_2O, but dissolves readily in both Et_2O and benzene. This solubility profile contrasts with that of Na[^{Mes}pic] (**2**), which is soluble in H_2O, but resists dissolution in low-polarity organic media.

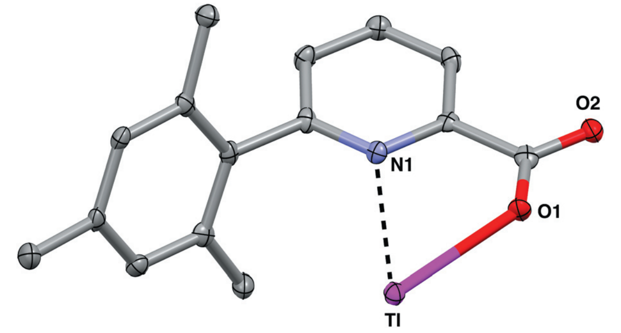

Fig. 1 Molecular structure of the monomeric portion of Tl(^{Mes}pic) (**5**). Selected bond distances (Å) and angles (°): Tl–O1 = 2.521(3); Tl–N1 = 2.792(3); N1–Tl–O1 = 61.73(9).

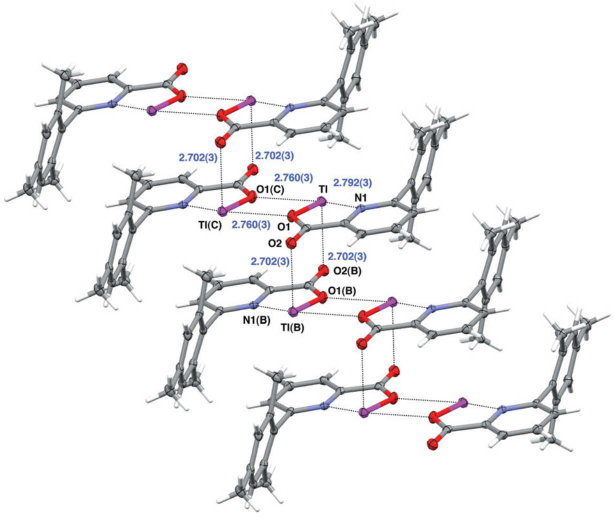

Fig. 2 Extended solid-state structure of Tl(^{Mes}pic) (**5**). Bond distances are in Å.

The ^{Mes}pic framework exhibits versatile coordination properties to both main-group and transition metal fragments. For example, a simple 1 : 1 complex between ^{Mes}pic and Tl(I) is formed upon treatment of Na[^{Mes}pic] (**2**) with thallium(I) triflate (TlOTf; OTf = O_3SCF_3) in a CH_2Cl_2–H_2O mixture (Scheme 1). The molecular structure of Tl(^{Mes}pic) (**5**) has been determined by X-ray diffraction (Fig. 1) and exhibits a primary interaction between one carboxylate-oxygen atom and the Tl center (d(Tl–O1) = 2.521(3) Å). The Tl–N(1) bond distance in the mononuclear portion of Tl(^{Mes}pic) (**5**) is considerably longer at 2.792(3) Å. Whereas low-coordinate complexes of Tl(I) containing monodentate, monoanionic ligands are known,[39,40] inspection of the lattice diagram reveals that Tl(^{Mes}pic) (**5**) adopts an extended 2-D staircase structure in the solid state (Fig. 2). In the extended structure, each Tl center makes close contacts with oxygen atoms from two neighboring ^{Mes}pic units and is best considered in an overall four-coordinate, *cis*-divacant octahedral geometry. Notably, the intermolecular contact between Tl and the

---

‡ The concentration dependence of the carboxylic acid proton chemical shift in ^{Mes}picH has not been determined.

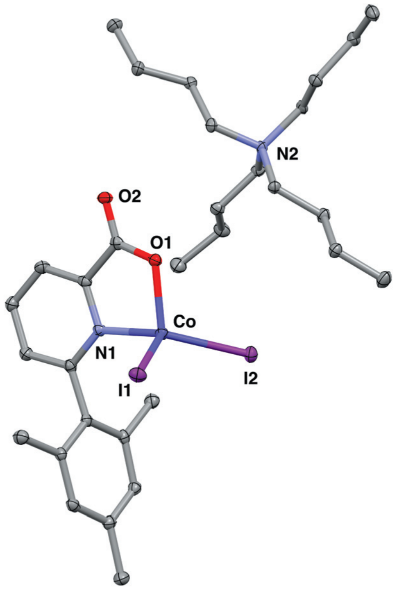

Fig. 3 Molecular structure of [NBu$_4$][CoI$_2$($^{\mathrm{Mes}}$pic)] (**6**). Selected bond distances (Å) and angles (°): Co–I1 = 2.5726(5); Co–I2 = 2.5675(5); Co–O1 = 1.964(2); Co–N1 = 2.062(3); O1–Co–N1 = 83.97(11); O1–Co–I1 = 112.55(7); O1–Co–I2 = 107.92(7); N1–Co–I1 = 109.72(8); N1–Co–I2 = 123.32(8); I1–Co–I2 = 115.030(19).

neighboring $^{\mathrm{Mes}}$pic carbonyl oxygen atom (*i.e.* Tl–O2(B)) is significantly shorter than the intramolecular Tl–N(1) contact (2.702 (3) *vs.* 2.792(3)). We believe this short contact likely manifests from the absence of a ligand *trans* to the carbonyl oxygen atom in the extended structure of Tl($^{\mathrm{Mes}}$pic) (**5**).

In addition to Tl(I) ions, a 1 : 1 complex is also formed between the $^{\mathrm{Mes}}$pic anion and the CoI$_2$ fragment. As shown in Scheme 1, combination of [NBu$_4$][$^{\mathrm{Mes}}$pic] (**4**) with 1.0 equiv. of cobalt(II) diiodide in THF solution leads to the paramagnetic salt [NBu$_4$][CoI$_2$($^{\mathrm{Mes}}$pic)] (**6**). Structural characterization of [NBu$_4$]-[CoI$_2$($^{\mathrm{Mes}}$pic)] (**6**, Fig. 3) revealed a four-coordinate Co center, which deviates significantly from an idealized tetrahedral geometry based on Houser's τ_4 geometry index (τ_4 = 0.86 for [NBu$_4$][CoI$_2$($^{\mathrm{Mes}}$pic)] (**6**) *vs.* 1.0 for idealized T_d).[41] Indeed, the coordination geometry of the cobalt center in the [CoI$_2$($^{\mathrm{Mes}}$pic)]$^-$ anion is best described as trigonal monopyramidal with an apical carboxylate oxygen atom and a near-trigonal, NI$_2$ plane ($\Sigma\angle_{(\mathrm{I–N–I})}$ = 347.06°). This geometry is likely a consequence of both the small bite angle of the $^{\mathrm{Mes}}$pic ligand (83.97(11)°) and minimization of steric interference between the iodide ligands and the encumbering mesityl group. Furthermore, unlike in the 1 : 1 adduct, Tl($^{\mathrm{Mes}}$pic) (**5**), close intermolecular contacts are not observed in the solid-state structure of [NBu$_4$][CoI$_2$($^{\mathrm{Mes}}$pic)] (**6**). While the large [NBu$_4$]$^+$ cation may obviate such interactions in the solid state, it is important to note that Evans Method magnetic moment determination of [NBu$_4$][CoI$_2$($^{\mathrm{Mes}}$pic)] (**6**) in CDCl$_3$ solution resulted in a μ_{eff} value of 4.4(1) μ_{B} (20 °C). The magnitude of this magnetic moment is consistent with a mononuclear d^7 Co center possessing an S = 3/2 ground state[42,43] and signifies that higher nuclearity species are likely not present to an appreciable extent in solution at room temperature.

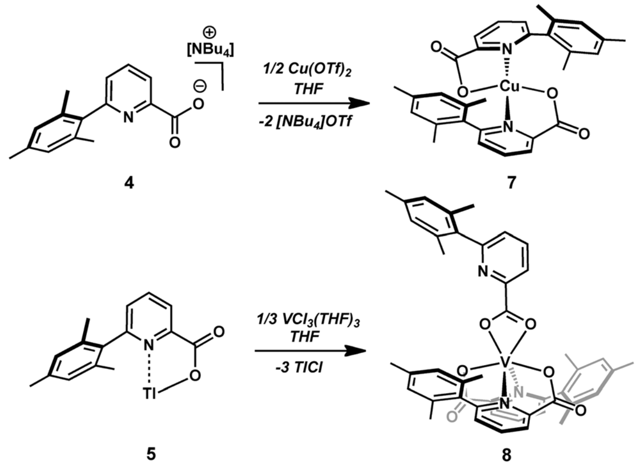

Scheme 2

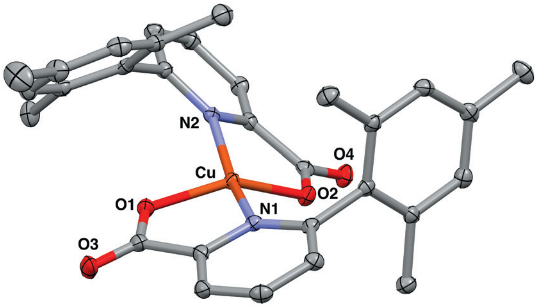

Fig. 4 Molecular structure of Cu($^{\mathrm{Mes}}$pic)$_2$ (**7**). Selected bond distances (Å) and angles (°): Cu–O1 = 1.909(2); Cu–O3 = 1.921(2); Cu–N1 = 1.980(2); Cu–N2 = 1.970(2); O1–Cu–O3 = 145.04(9); N1–Cu–N2 = 161.97(9); O1–Cu–N2 = 97.97(9); O3–Cu–N2 = 84.08(9); O1–Cu–N1 = 85.10(9); O3–Cu–N1 = 103.61(9).

In addition to the 1 : 1 $^{\mathrm{Mes}}$pic complexes of Tl(I) and the CoI$_2$ fragment, a neutral bis-$^{\mathrm{Mes}}$pic complex of Cu(II) can be readily prepared and its molecular structure further demonstrates the steric encumbrance posed by the 6-position mesityl group. Treatment of Cu(II) triflate (Cu(OTf)$_2$) with 2.0 equiv. of [NBu$_4$]-[$^{\mathrm{Mes}}$pic] (**4**) in Et$_2$O results in the precipitation of the paramagnetic bis-picolinate complex, Cu($^{\mathrm{Mes}}$pic)$_2$ (**7**), as a blue solid (Scheme 2). Evans Method magnetic moment determination in C$_6$D$_6$ solution (20 °C) gave rise to a μ_{eff} value of 1.83(8) μ_{B}, which is close to the spin-only value expected for a d^9 Cu(II) center. Accordingly, crystallographic analysis of Cu($^{\mathrm{Mes}}$pic)$_2$ (**7**) revealed a discrete four-coordinate mononuclear Cu center unperturbed by secondary interactions from neighboring molecules. Most interestingly, however, the Cu atom within Cu ($^{\mathrm{Mes}}$pic)$_2$ (**7**) adopts a C_2-symmetric, seesaw geometry (Fig. 4). Metrical parameters in support of this claim for Cu($^{\mathrm{Mes}}$pic)$_2$ (**7**) include a bent O1–Cu–O2 angle of 145.04(9)° and a relatively more linear angle of 161.97(9)° between the *trans*-oriented N1 and N2 atoms. This seesaw geometry is in sharp contrast to the undistorted square-planar geometry observed for the unsubstituted bis-picolinate complex Cu(pic)$_2$.§ The structure of Cu(pic)$_2$ has been reported by several groups.[44–50] Each determination has shown a *trans* orientation of the pyridyl units similar

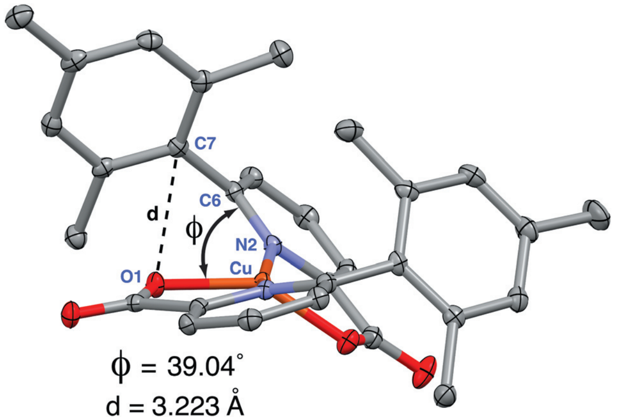

Fig. 5 Alternative view of the molecular structure of Cu(^{Mes}pic)$_2$ (**7**) emphasizing the C6–N2–Cu–O1 dihedral angle of 39.04° and the seesaw Cu coordination geometry.

to that found for Cu(^{Mes}pic)$_2$ (**7**), but with 180° angles between both the Cu-coordinated nitrogen and oxygen atoms. Accordingly, we believe the distortion observed for Cu(^{Mes}pic)$_2$ (**7**) relative to Cu(pic)$_2$ results to alleviate steric interactions between the 6-Mes substituent and the Cu-coordinated oxygen atom. As shown in Fig. 5, the C6–N2–Cu–O1 dihedral angle in Cu(^{Mes}pic)$_2$ (**7**) is 39.04°, which affords a 3.223 Å separation between O1 and the *ipso*-mesityl carbon atom C7. In a nominally square-planar configuration, this separation within Cu(^{Mes}pic)$_2$ (**7**) would undoubtedly be shorter, leading to an unfavorable close contact between the coordinated O atom and the mesityl-ring π-face. Thus, as hoped, judicious placement of an encumbering substituent in the 6-position of the 2-picolinate framework can force an entatic[51] metal-center coordination geometry relative to unhindered picolinate variants.

Tris-^{Mes}pic complexes also exhibit different structural and coordination properties relative to their less hindered analogues due to the presence of the encumbering Mes group. As shown in Scheme 2, the treatment of VCl$_3$(THF)$_3$ with 3.0 equiv. of the thallium(I) complex, Tl(^{Mes}pic) (**5**), in THF solution results in the precipitation of TlCl and formation of the paramagnetic tris-picolinato complex V(^{Mes}pic)$_3$ (**8**). The latter gives rise to a solution magnetic moment of 2.7(1) μ_B (C_6D_6, 20 °C), which is reflective of an $S = 1$, d^2 vanadium center. Structural characterization of V(^{Mes}pic)$_3$ (**8**, Fig. 6) revealed two *trans*-pyridyl, ^{Mes}pic ligands exhibiting the typical κ^2-*N*,*O* coordination mode. However, the third ^{Mes}pic ligand binds the vanadium center in a κ^2-*O*$_2$ fashion *via* the carboxylate group and possesses a non-coordinated pyridyl unit. This 2 : 1 κ^2-*N*,*O* : κ^2-*O*$_2$ coordination mode is unique among homoleptic tris-2-picolinate complexes of the 3d-metals. Indeed, the isostructural complexes V(pic)$_3$,[52] Cr(pic)$_3$,[53] Mn(pic)$_3$[54] and Co(pic)$_3$[55] exhibit three, mutually κ^2-*N*,*O*-coordinated unsubstituted 2-picolinate ligands. As with the distortion observed for Cu(^{Mes}pic)$_2$ (**6**), steric pressures between the 6-position mesityl group and the coordinated oxygen atoms, or interference between the Mes groups themselves, may be reasonably assumed to inhibit a third ligand from adopting a κ^2-*N*,*O* coordination mode in V(^{Mes}pic)$_3$ (**8**). Given that tight κ^2-*N*,*O* chelation is a hallmark of the 2-picolinate ligand, it is interesting to speculate that steric destabilization of this binding mode, as illustrated within the structure of V(^{Mes}pic)$_3$ (**8**), may lead to enhanced reactivity for an otherwise kinetically inert metal system.[52]

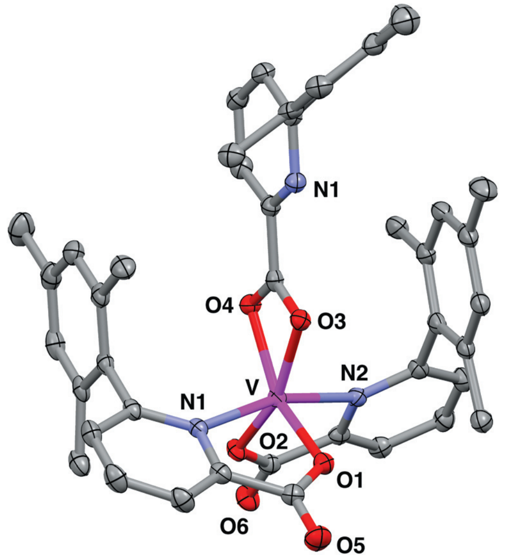

Fig. 6 Molecular structure of V(^{Mes}pic)$_3$ (**8**). Selected bond distances (Å) and angles (°): V–O1 = 1.908(2); V–O2 = 1.909(2); V–O3 = 2.052(2); V–O4 = 2.062(2); V–N1 = 2.158(3); V–N2 = 2.151(3); N1–V–N2 = 159.87(10); O1–V–O2 = 103.60(10); O1–V–O4 = 158.09(10); O2–V–O3 = 160.66(9); O3–V–O4 = 63.55(9); O3–V–N1 = 105.47(10); O4–V–N2 = 104.12(11); N1–V–N2 = 159.87(10).

Conclusions

The coordination chemistry of the 2-picolinate anion is well developed and has been exploited for numerous applications. We have shown here that these established coordination properties can be further modulated by placement of an encumbering mesityl group at the 6-position of the 2-picolinate framework. The 6-mesityl-2-picolinate anion, [^{Mes}pic]$^-$, can be synthesized in two steps from readily available starting materials and several useful derivatives are prepared by straightforward procedures. Most importantly, [^{Mes}pic]$^-$ functions as a ligand to both main-group and transition-metal fragments. As demonstrated by the Cu(II) complex, Cu(^{Mes}pic)$_2$ (**7**), steric interference between the flanking mesityl substituents and a metal-coordinated oxygen atom can lead to pronounced structural distortions. In this case, the Cu center in Cu(^{Mes}pic)$_2$ (**7**) adopts a C_2-symmetric, seesaw coordination geometry, rather than a square-planar geometry as found for the unhindered, parent picolinate complex Cu(pic)$_2$.[44–50] Additionally, the tris-^{Mes}pic complex V(^{Mes}pic)$_3$

---

§ It is important to note that the unsolvated (ref. 44 and 45) and monohydrate (ref. 46–49) forms of Cu(pic)$_2$ feature close intermolecular separations between the Cu center and carbonyl oxygen atoms from two neighboring molecules. These intermolecular distances are long (2.770(8) Å and 2.814(4) Å, respectively), but non-negligible. Similar close contacts are not observed in the solid-state structure of Cu(^{Mes}pic)$_2$ (**7**). For comparison, the closest intermolecular contact between the Cu center in Cu(^{Mes}pic)$_2$ (**7**) and a neighboring carbonyl oxygen atom is 7.390 Å.

(**8**) features a κ^2-O_2-coordinated ligand in the solid-state, which is atypical of 3d-metal M(pic)$_3$ complexes.[52–55] This structural outcome is notable, as it indicates that alleviation of steric pressures around the metal coordination sphere outweighs the thermodynamic preference for formation of a third, five-membered chelate ring. Accordingly, further investigations into the effect of sterically-induced structural modulation on the reactivity of these, and other, $^{\mathrm{Mes}}$pic-containing complexes are in progress.

Experimental section

General considerations

Unless otherwise stated, all manipulations were carried out under an atmosphere of dry dinitrogen using standard Schlenk and glovebox techniques. Solvents were dried and deoxygenated according to standard procedures.[56] Reagent grade starting materials were purchased from commercial sources and were used as received or purified by standard procedures.[57] Benzene-d_6 (Cambridge Isotope Laboratories) was degassed and stored over 4 Å molecular sieves for 2 d prior to use. Celite 405 (Fisher Scientific) was dried under vacuum (24 h) at a temperature above 250 °C and stored in the glovebox prior to use. Solution ^{1}H and ^{13}C{^{1}H} spectra were recorded on Varian Mercury 300 and 400 spectrometers, a Varian X-Sens500 spectrometer, or a JEOL ECA-500 spectrometer. ^{1}H and ^{13}C{^{1}H} chemical shifts are reported in ppm relative to SiMe$_4$ (^{1}H and ^{13}C $\delta = 0.0$ ppm) with reference to residual-protio resonances of 7.16 ppm (^{1}H) and 128.06 ppm (^{13}C) for benzene-d_6, and 7.26 ppm (^{1}H) and 77.16 ppm (^{13}C) for CDCl$_3$. FTIR spectra were recorded on a Thermo-Nicolet iS10 FTIR spectrometer. Samples were prepared as KBr pellets. The following abbreviations were used for the intensities and characteristics of important IR absorption bands: vs = very strong, s = strong, m = medium, w = weak, vw = very weak; b = broad, vb = very broad, sh = shoulder. High resolution mass spectrometry (HRMS) was performed using an Agilent 6230 ESI-TOFMS instrument in either positive or negative ion mode as necessary. Combustion analyses were performed by Robertson Microlit Laboratories of Ledgewood, NJ (USA).

Synthesis of methyl 6-mesityl-2-picolinate ($^{\mathrm{Mes}}$picMe, 1)

In the glovebox, tris(dibenzylideneacetone)dipalladium(0)-(Pd$_2$(dba)$_3$; 0.060 g, 0.066 mmol, 1.4 mol%), tricyclohexylphosphine (PCy$_3$; 0.040 g, 0.144 mmol, 3.1 mol%), and K$_3$PO$_4$ (1.85 g, 8.19 mmol, 1.8 equiv.) were placed in a 100 mL airtight reaction vessel. On the Schlenk line, under an argon blanket, methyl 6-bromopyridine-2-carboxylate (1.00 g, 4.62 mmol), mesitylboronic acid (MesB(OH)$_2$; 1.00 g, 6.1 mmol, 1.3 equiv.) and toluene (20 mL) were added to the reaction vessel and sealed. The reaction mixture was heated in an oil bath at 100 °C for 24 h. Upon cooling, 50 mL of a saturated aqueous sodium bicarbonate solution and 40 mL of diethyl ether were added to the mixture and stirred for 1 h. The organic and aqueous layers were separated, and the aqueous layer extracted with Et$_2$O (2 × 100 mL). The combined organic layers were dried over magnesium sulfate and evaporated to dryness, which yielded a colorless solid. Yield: 0.810 g, 3.19 mmol, 70%. This material can be used without further purification. However, purification can be achieved either by crystallization from Et$_2$O or by flash chromatography, using 10 : 90 EtOAc : hexanes on basic silica. ^{1}H NMR (400.6 MHz, CDCl$_3$, 20 °C): $\delta = 8.10$ (dd, 1H, $J = 8$ Hz, 1 Hz), 7.89 (t, 1H, $J = 8$ Hz, *p*-Py), 7.40 (dd, 1H, $J = 8$ Hz, 1 Hz), 6.91 (s, 1H, *m*-Mes), 3.99 (s, 3H, CO$_2$CH_3), 2.31 (s, 3H, *p*-CH_3), 2.01 (s, 6H, *o*-CH_3) ppm. ^{13}C{^{1}H} NMR (100.6 MHz, CDCl$_3$, 20.6 °C): 166.3, 160.5, 148.2, 137.9, 137.2, 137.1, 128.5, 128.4, 123.3, 53.1 (CO$_2$$CH_3$), 21.2 (*o*-CH$_3$), 20.4 (*p*-CH$_3$) ppm. FTIR (KBr pellet, cm^{-1}) $\nu = 3065$ (w), 2960 (m), 2918 (m), 2856 (m), 2730 (w), 1722 (s, ν_{CO}), 1677 (w), 1611 (m), 1584, 1565 (m), 1456, 1379 (m), 1272 (m), 1235, 1083, 1055, 991, 855 (m). HRMS (ESI) *m*/*z* Found: 256.1332 [M + H]$^+$.

Synthesis of sodium 6-mesityl-2-picolinate (Na[$^{\mathrm{Mes}}$pic], 2)

To an Et$_2$O solution of methyl 6-mesitylpyridine-2-carboxylate ($^{\mathrm{Mes}}$picMe (**1**); 0.810 g, 3.17 mmol, 90 mL) was added 8 mL of a 2 M methanolic solution of NaOH (16.0 mmol, 5.0 equiv.). The reaction mixture was stirred for 1 h, resulting in the formation of a colorless precipitate. The reaction mixture was diluted with Et$_2$O (100 mL), filtered, and the resulting solid washed with Et$_2$O (1 × 50 mL) and *n*-pentane (1 × 50 mL). The resulting colorless solid was collected and dried *in vacuo* overnight. Yield: 0.812 g, 2.92 mmol, 92%. ^{1}H NMR (400.6 MHz, D$_2$O, 20 °C): $\delta = 7.94$ (t, 1H, $J = 8$ Hz) 7.78 (d, 1H, $J = 8$ Hz, *p*-Py), 7.29 (d, 1H, $J = 8$ Hz), 7.01 (s, 1H, *m*-Mes), 2.28 (s, 3H, *p*-CH_3), 1.92 (s, 6H, *o*-CH_3) ppm. ^{13}C{^{1}H} NMR (100.6 MHz, D$_2$O with methanol-d_4 internal standard, 20 °C): 175.0, 160.1, 140.0, 139.8, 137.8, 127.9, 123.1, 21.6 (*o*-CH$_3$), 20.6 (*p*-CH$_3$) ppm. FTIR (KBr pellet, cm^{-1}) $\nu = 2973$ (m), 2942 (m), 2919 (m), 2857 (w), 2729 (w), 1621 (s, ν_{CO}), 1578 (s, ν_{CO}), 1562, 1449 (m), 1430 (m), 1377, 1231 (w), 1172 (w), 1081 (w), 1059 (w), 995 (w), 867 (m), 784, 749 (m), 659 (m). HRMS (ESI) *m*/*z* Found: 240.1031 [M]$^-$.

Synthesis of 6-mesityl-2-picolinic acid ($^{\mathrm{Mes}}$picH, 3)

To an acetone slurry of sodium 6-mesitylpyridine-2-carboxylate (Na[$^{\mathrm{Mes}}$pic] (**2**); 0.522 g, 1.88 mmol) was added aqueous HCl (12 M, 0.156 mL, 1.88 mmol, 1.0 equiv.) *via* syringe. The mixture was placed in an ultrasonic bath for 40 min, which resulted in full dissolution of all precipitates. The resulting solution was then filtered through Celite and all volatiles were removed from the filtrate *in vacuo* to yield a colorless solid. Yield: 0.330 g, 1.29 mmol, 69%. ^{1}H NMR (400.6 MHz, CDCl$_3$, 20 °C): $\delta = 10.76$ (s, 1H, CO$_2$$H$), 7.87 (dd, 1H, $J = 8$ Hz, 1 Hz), 6.91 (t, 1H, $J = 8$ Hz, *p*-Py), 6.79 (s, 1H, *m*-Mes), 6.66 (dd, 1H, $J = 8$ Hz, 1 Hz), 2.16 (s, 3H, *p*-CH_3), 1.79 (s, 6H, *o*-CH_3) ppm. ^{13}C{^{1}H} NMR (100.6 MHz, CDCl$_3$, 20 °C): 163.6, 158.9, 146.6, 138.5, 138.3, 135.7, 121.6, 21.1 (*o*-CH$_3$), 20.2 (*p*-CH$_3$) ppm. FTIR (KBr pellet, cm^{-1}) $\nu = 3088$ (m), 2922, 2855 (m), 2731 (m), 2485 (m, vb $\nu_{\mathrm{(OH)}}$), 1730 (s, ν_{CO}), 1684 (w), 1625 (m), 1610 (m), 1587 (m), 1515 (w), 1448 (m), 1290 (m), 1261 (m), 1226, 1175 (m), 2085 (m), 1032 (w), 1002 (m), 842 (m), 777 (m), 709 (m). HRMS (ESI) *m*/*z* Found: 242.1175. [M + H]$^+$.

Synthesis of terabutylammonium 6-mesityl-2-picolinate ([NBu_4]-[^{Mes}pic], 4)

To a slurry of ^{Mes}picH (**3**) in H_2O (0.300 g, 1.24 mmol, 4 mL) was added [NBu_4]$OH{\cdot}30H_2O$ (1.50 g, 1.87 mmol, 1.5 equiv.), followed by 10 mL of CH_2Cl_2. The reaction mixture was stirred for 1 h. The organic and aqueous layers were then separated and the aqueous layer was washed with CH_2Cl_2 (3 × 20 mL). The organic layers were combined and dried under reduced pressure. The resulting oily residue was placed in a vacuum desiccator with phosphorus pentoxide for 2 d. The resulting solid was then transferred to a glovebox, slurried in Et_2O and then dried thoroughly *in vacuo*. Recrystallization from a THF–Et_2O mixture at −35 °C produced a colorless solid, which was collected and dried *in vacuo*. Yield: 0.382, 0.794 mmol 64%. ^{1}H NMR (400.6 MHz, C_6D_6, 20 °C): δ = 8.55 (dd, 1H, *J* = 8 Hz, 1 Hz), 7.37 (t, 1H, *J* = 8 Hz), 6.84 (s, 1H, *m*-Mes), 6.82 (d, 1H, *J* = 1 Hz), 3.48 (m, 8H, NBu_4 NCH_2), 2.21 (s, 3H, *p*-Mes CH_3), 2.13 (s, 6H, *o*-Mes CH_3), 1.60 (m, 8H, NBu_4 methylene), 1.34 (m, 8H, NBu_4 methylene), 0.95 (t, 12H, *J* = 7.2 Hz, NBu_4 CH_3) ppm. $^{13}C\{^1H\}$ NMR (100.6 MHz, $CDCl_3$, 20 °C): 169.36, 161.9, 157.9, 140.3, 136.1, 135.4, 128.5, 123.0, 122.7, 58.5, 24.2, 21.2, 20.8, 20.3, 14.2 ppm. FTIR (KBr pellet, cm^{-1}) ν = 2956, 2870, 2372 (w), 1619 (s, ν_{CO}), 1574 (s, ν_{CO}), 1491 (m), 1480 (m), 1394 (m), 1949, 1280 (w), 1229 (w), 1165 (m), 1150 (m), 1074 (m), 1058 (m), 1030 (m), 989 (m), 885 (m), 854 (m), 738, 654 (m). HRMS (ESI) *m*/*z* Found: 240.1032 $[M]^-$.

Synthesis of thallium(I) 6-mesityl-2-picolinate (Tl(^{Mes}pic), 5)

To an aqueous solution of Na[^{Mes}pic] (**2**, 0.842 g, 3.20 mmol, 4 mL) was added an aqueous solution of thallium(I) triflate (TlOTf; 1.200 g, 3.39 mmol, 1.05 equiv., 4 mL), followed by 40 mL of CH_2Cl_2. The mixture was stirred for 1 h, after which the organic and aqueous layers were separated. The aqueous layer was then extracted with CH_2Cl_2 (3 × 100 mL). The combined organic layers were evaporated to dryness and the resulting residue dissolved in 10 mL of CH_2Cl_2. 50 mL of *n*-pentane were then added, resulting in the precipitation a colorless solid, which was collected and dried *in vacuo*. Yield: 1.10 g, 2.47 mmol, 77%. Single-crystal X-ray diffraction quality crystals were grown from a saturated toluene–$CHCl_3$ (10 : 1) mixture at −35 °C. ^{1}H NMR (400.6 MHz, $CDCl_3$, 20 °C): δ = 7.93 (d, 1H, *J* = 7 Hz, 1 Hz), 7.83 (t, 1H, *J* = 7 Hz, *p*-Py), 7.30 (d, 1H, *J* = 7 Hz), 6.96 (s, 1H, *m*-Mes), 2.34 (s, 3H, *p*-CH_3), 2.00 (s, 6H, *o*-CH_3) ppm. $^{13}C\{^1H\}$ NMR (100.6 MHz, $CDCl_3$, 20 °C): 172.7, 157.4, 155.0, 138.5, 138.2, 136.1, 135.9, 128.7, 126.7, 123.8, 21.3 (*o*-CH_3), 20.5 (*p*-CH_3) ppm. FTIR (KBr pellet, cm^{-1}) ν = 3065 (w), 2948 (m), 2917 (m), 2856 (w), 2732 (w), 1596 (s, ν_{CO}), 1570 (s, ν_{CO}), 1488 (w), 1453 (m), 1396 (m), 1378 (m), 1360, 1280 (w), 1236 (m), 1172 (w), 1150 (w), 1080 (m), 1057 (m), 1033 (w), 998 (m), 852 (m), 840 (m), 776, 753 (m), 734 (m), 660 (m). Anal. calcd for $TlC_{15}NO_2H_{14}$: C, 40.52; H, 3.17; N, 3.15. Found: C, 40.35; H, 3.01; N, 3.23.

Synthesis of [NBu_4][CoI_2(^{Mes}pic)] (6)

To a THF solution of CoI_2 (0.026 g, 0.082 mmol, 3 mL) was added a THF solution of [NBu_4][^{Mes}pic] (**4**; 0.040 g, 0.082 mmol, 1.0 equiv., 2 mL). The mixture was stirred for 30 min while changing in color from green to teal. The reaction mixture was then filtered through Celite, layered with Et_2O and cooled to −35 °C for 12 h to produce a teal solid that was collected and dried *in vacuo*. Yield: 0.049 g, 0.061 mmol, 74%. Single-crystal X-ray diffraction quality crystals of NBu_4[CoI_2Ar-MesPic]$\cdot C_6H_6$ were grown from diffusion of *n*-pentane into a saturated benzene solution at room temperature. ^{1}H NMR (400.6 MHz, $CDCl_3$, 20 °C): δ = 35.9 (s), 11.7 (s), 4.8 (s), 3.5 (s), 2.2 (s), −0.45 (s), −2.6 (s), −5.2 (s), −9.0 (s), −22.7 (s) ppm. FTIR (KBr pellet, cm^{-1}) ν = 2958, 2873 (m), 2732 (w), 1655 (s, ν_{CO}), 1610 (m), 1593, 1564 (w), 1488 (m), 1460 (m), 1377 (m), 1341 (m), 1242 (m), 1157 (m), 1080 (m), 1060 (m), 1021 (m), 880 (w), 866 (w), 848 (w), 780 (m), 760 (m), 740 (m), 675 (w). μ_{eff} (Evans method, 500 MHz, $CDCl_3$ with $O(SiMe_3)_2$, 20 °C) = 4.4 (±0.1) μ_B (average of 5 independent measurements) Anal. calcd for $CoI_2C_{31}N_2O_2H_{50}$: C, 46.81; H, 6.34; N, 3.52. Found: C, 46.24; H, 5.55; N, 3.26.

Synthesis of Cu(^{Mes}pic)$_2$ (7)

To an Et_2O solution of $CuOTf_2$ (0.026 g, 0.072 mmol, 3 mL) was added an Et_2O slurry of [NBu_4][^{Mes}pic] (**4**; 0.070 g, 0.14 mmol, 2.0 equiv., 5 mL). The reaction mixture was stirred for 36 h, resulting in the formation of a blue precipitate. The reaction mixture was filtered and the resulting solid extracted with THF (2 mL). Layering this solution with *n*-pentane, followed by storage at −35 °C for 12 h produced single-crystal X-ray diffraction quality crystals. Yield: 0.030 g, 0.054 mmol, 75%. ^{1}H NMR (400.6 MHz, $CDCl_3$, 20 °C): δ = 9.1 (s), 6.8 (s), 3.3 (s, very broad), 1.7 (s) ppm. FTIR (KBr pellet, cm^{-1}) ν = 3073 (w), 2920 (m), 2857 (m), 2734 (w), 1674 (s, ν_{CO}), 1599, 1563 (m), 1460, 1396 (m), 1377 (m), 1330, 1301 (m), 1279 (m), 1242, 1179 (m), 1148, 1077 (m), 1029 (m), 871 (m), 789, 767 (m), 861 (m), 595 (w). μ_{eff} (Evans method, 500 MHz, $CDCl_3$ with $O(SiMe_3)_2$, 20 °C) = 1.83 (±0.08) μ_B (average of 4 independent measurements). Anal. calcd for $CuC_{30}N_2O_4H_{28}$: C, 66.22; H, 5.19; N, 5.15. Found: C, 65.88; H, 5.15; N, 5.01.

Synthesis of V(Ar^{Mes}Pic)$_3$ (8)

To a THF solution of $VCl_3(THF)_3$ [58] (0.042 g, 0.112 mmol, 6 mL) was added a THF solution of Tl(^{Mes}pic) (**5**, 0.150 g, 0.336 mmol, 3.0 equiv., 4 mL). The reaction mixture was stirred for 2 h, resulting in the formation of a colorless precipitate. The mixture was then filtered through Celite and all volatile materials were removed under reduced pressure. The resulting green residue was dissolved in toluene, layered with pentane and stored at −35 °C overnight to afford green crystals. Yield: 0.050 mg, 0.063 mmol, 56%. Single-crystal X-ray diffraction quality crystals of V(^{Mes}pic)$_3\cdot$THF were grown by diffusion of *n*-pentane into a saturated THF solution. ^{1}H NMR (400.6 MHz, C_6D_6, 20 °C): δ = 24.1, 19.2, 10.7, 8.2, 6.7 (s), 3.5 (s, very broad), 3.1 (s), −6.6 (s), −18.8 (s) ppm. FTIR (KBr pellet, cm^{-1}) ν = 3069 (w), 3003 (m), 2956 (m), 2920 (m), 2858 (m), 2734 (w), 1707 (s, ν_{CO}), 1690 (s, ν_{CO}), 1610 (m), 1599 (m), 1564 (m), 1516 (m), 1474 (m), 1460 (m), 1420 (m), 1382 (m), 1319, 1300 (m), 1273 (m), 1229 (m), 1162 (m), 1146, 1084 (m),

Table 1 Crystallographic data and refinement information

	$Tl(^{Mes}pic)$ (**5**)	$[NBu_4][CoI_2(^{Mes}pic)]$ (**6**·C_6H_6)	C_6H_6 $Cu(^{Mes}pic)2$ (**7**)	$V(^{Mes}pic)_3$·THF (**8**·THF)
Formula	$C_{15}H_{14}NO_2Tl$	$C_{37}H_{56}CoI_2N_2O_2$	$C_{30}H_{28}CuN_2O_4$	$C_{49}H_{50}N_3O_7V$
Crystal System	Monoclinic	Triclinic	Orthorhombic	Monoclinic
Space Group	$P2_1/n$	$P\bar{1}$	$Pca2_1$	$P2_1/n$
a/Å	5.4362(3)	9.7875(6)	19.0917(14)	11.7453(16)
b/Å	14.4583(7)	11.8633(7)	7.7213(6)	12.1951(15)
c/Å	17.0112(9)	18.2575(10)	17.8169(13)	29.336(4)
α (°)	90	101.7360(10)	90	90
β (°)	94.3580(10)	102.8450(10)	90	96.980(7)
γ (°)	90	103.3080(10)	90	90
V/Å^3	1333.18(12)	1937.6(2)	2626.4(3)	4170.9(9)
Z	4	2	4	4
Radiation, λ/Å	Mo Kα, 0.71073	Mo Kα, 0.71073	Mo Kα, 0.71073	Mo Kα, 0.71073
ρ (calcd) g cm^{-3}	2.215	1.497	1.376	1.344
μ (Mo Kα), mm^{-1}	12.111	2.068	0.870	0.295
Temperature/K	100(2)	100(2)	100(2)	100(2)
θ max (°)	25.46	25.45	25.47	25.82
data/parameters	2480/175	7117/404	4126/340	7987/550
R_1	0.0200	0.0320	0.0294	0.0620
wR_2	0.0429	0.0648	0.0688	0.0931
GOF	1.031	1.036	1.035	1.022

1056 (m), 1016 (m), 990 (w), 879 (m), 847 (m), 768, 667 (m), 660 (m). μ_{eff} (Evans method, 500 MHz, C_6D_6 with $O(SiMe_3)_2$, 20 °C) = 2.7 (±0.1) μ_B (average of 5 independent measurements). Repeated attempts to obtain satisfactory combustion analysis on single crystals of $V(^{Mes}pic)_3$·THF were unsuccessful. These attempts consistently resulted in low carbon analysis, which is likely due to small amounts of residual TlCl.

Crystallographic structure determinations

Single-crystal X-ray structure determinations were carried out at low temperature on a Bruker P4, Platform or Kappa Diffractometer equipped with a Bruker APEX detector. All structures were solved by direct methods with SIR 2004[59] and refined by full-matrix least-squares procedures utilizing SHELXL-97.[60] Crystallographic data-collection and refinement information is listed in Table 1.

Acknowledgements

We thank the California Institute of Telecommunications and Information Technology (CalIT^2) for an undergraduate research scholarship to P.W.S. We also gratefully acknowledge the U.S. National Science Foundation for support through a CAREER Award (CHE-0954710) and NMR instrumentation grants to the UCSD Department of Chemistry and Biochemistry (CHE-0741968 and CHE-9709183). J.S.F. is an Alfred P. Sloan Research Fellow (2011–2013) and a Cottrell Scholar of Research Corporation (2010–2012).

Notes and references

1 X. S. Tan, Z. S. Ma, N. C. Shi, D. G. Fu, J. Chen and W. X. Tang, *J. Chem. Soc., Dalton Trans.*, 1996, 2735–2738.
2 D. Huang, W. Wang, X. Zhang, C. Chen, F. Chen, Q. Liu, D. Liao, L. Li and L. Sun, *Eur. J. Inorg. Chem.*, 2004, 1454–1464.
3 C. Biswas, P. Mukherjee, M. G. B. Drew, C. J. Gómez-García, J. M. Clemente-Juan and A. Ghosh, *Inorg. Chem.*, 2007, **46**, 10771–10780.
4 C. Biswas, A. D. Jana, M. G. B. Drew, G. Mostafa and A. Ghosh, *Polyhedron*, 2009, **28**, 653–660.
5 J. E. Powell and J. W. Ingemanson, *Inorg. Chem.*, 1968, **7**, 2459–2461.
6 N. B. Keck, N. J. Hornung and W. G. Bos, *J. Inorg. Nucl. Chem.*, 1974, **36**, 1521–1525.
7 T. E. Eriksen, I. Grenthe and I. Puigdomenech, *Inorg. Chim. Acta*, 1987, **126**, 131–135.
8 While $Cr(pic)_3$ is commercially available as a dietary supplement, the standing of chromium as an essential trace mineral in mammalian metabolism is controversial. See J. B. Vincent, *Dalton Trans.*, 2010, **39**, 3787–3794 and references therein.
9 S. A. Richert, P. K. S. Tsang and D. T. Sawyer, *Inorg. Chem.*, 1989, **28**, 2471–2475.
10 See for example, E. Libby, R. J. Webb, W. E. Streib, K. Folting, J. B. Huffman, D. N. Hendrickson and G. Christou, *Inorg. Chem.*, 1989, **28**, 4037–4040.
11 For representative reviews, see: (*a*) D. H. R. Barton and D. Doller, *Acc. Chem. Res.*, 1992, **25**, 504–512; (*b*) D. H. R. Barton and B. M. Chabot, *Tetrahedron*, 1997, **53**, 487–510.
12 D. P. O'Malley, J. Yamaguchi, I. S. Young, I. B. Seiple and P. S. Baran, *Angew. Chem., Int. Ed.*, 2008, **47**, 3581–3583.
13 S. Su, I. B. Seiple, I. S. Young and P. S. Baran, *J. Am. Chem. Soc.*, 2008, **130**, 16490–16491.
14 I. B. Seiple, S. Su, I. S. Young, C. A. Lewis, J. Yamaguchi and P. S. Baran, *Angew. Chem., Int. Ed.*, 2010, **49**, 1095–1098.
15 Following Baran's reports of silver(II)-mediated hydroxylation (ref. 12–14), $Ag(pic)_2$ has become commercially available from Sigma-Aldrich Chemical Co. (Cat. # 718157).
16 W. R. Gutekunst and P. S. Baran, *Chem. Soc. Rev.*, 2011, **40**, 1976–1991.
17 I. B. Seiple, S. Su, R. A. Rodriguez, R. Gianatassio, Y. Fujiwara, A. L. Sobel and P. S. Baran, *J. Am. Chem. Soc.*, 2010, **132**, 13194–13196.
18 (*a*) J. B. Lee and T. G. Clarke, *Tetrahedron Lett.*, 1967, **8**, 415–422; (*b*) T. G. Clarke, N. A. Hampson, J. B. Lee, J. R. Morley and B. Scanlon, *Can. J. Chem.*, 1969, **47**, 1649–1645.
19 T. G. Clarke, N. A. Hampson, J. B. Lee, J. R. Morley and B. Scanlon, *J. Chem. Soc. C*, 1970, 815–817.
20 For additional early uses of $Ag(pic)_2$ as an oxidant, see: (*a*) L. Syper, *Tetrahedron Lett.*, 1967, **8**, 4193–4198; (*b*) J. M. Anderson and J. K. Kochi, *J. Org. Chem.*, 1970, **35**, 986–989.
21 E. G. Cox, W. Wardlaw and K. C. Webster, *J. Chem. Soc. A*, 1936, 775–781.
22 J. A. McMillan, *Chem. Rev.*, 1962, **62**, 65–80.
23 H. G. Hecht and J. P. Frazier, *J. Inorg. Nucl. Chem.*, 1967, **29**, 613–618.
24 G. W. A. Fowles, R. W. Matthews and R. A. Walton, *J. Chem. Soc. A*, 1968, 1108–11143.
25 M. G. B. Drew, G. W. A. Fowles, R. W. Matthews and R. A. Walton, *J. Am. Chem. Soc.*, 1969, **91**, 7769–7771.

26 M. G. B. Drew, R. W. Matthews and R. A. Walton, *J. Chem. Soc. A*, 1970, 1405–1410.
27 J. L. Hoare, K. J. Cavell, R. Hecker, B. W. Skelton and A. H. White, *J. Chem. Soc., Dalton Trans.*, 1996, 2197–2205.
28 À. Leiva, W. Clegg, L. Cucurull-Sánchez, P. González-Duarte and J. Pons, *J. Chem. Crystallogr.*, 1999, **29**, 1097–1101.
29 G.-H. Xu, J.-F. Ma, Y.-Y. Liu and S.-L. Li, *Acta Crystallogr., Sect. C: Cryst. Struct. Commun.*, 2006, **62**, m581–m583.
30 A. A. Rachford, J. L. Petersen and J. J. Rack, *Inorg. Chem.*, 2006, **45**, 5953–5960.
31 B.-M. Kukovec, Z. Popović, B. Kozlevcar and Z. Jaglicic, *Polyhedron*, 2008, **27**, 3631–3638.
32 B.-M. Kukovec, P. D. Vaz, Z. Popović, M. J. Calhorda, K. Furić, G. Pavlović and M. R. Linarić, *Cryst. Growth Des.*, 2008, **8**, 3465–3473.
33 B.-M. Kukovec, Z. Popovic, S. Komorsky-Lovric, V. Vojkovic and M. Vinkovic, *Inorg. Chim. Acta*, 2009, **362**, 2704–2714.
34 T. Sasagawa, Y. Yoshikawa, K. Kawabe, H. Sakurai and Y. Kojima, *J. Inorg. Biochem.*, 2002, **88**, 108–112.
35 Y. Kojima, Y. Yoshikawa, E. Ueda, N. Kishimoto, M. Tadokoro and H. Sakurai, *Bull. Chem. Soc. Jpn.*, 2005, **78**, 451–455.
36 The complex $\mathrm{Mn}({}^{\mathrm{i\text{-}Pr}}\mathrm{pic})_2(\mathrm{OH}_2)_2$, containing the 6-${}^{\mathrm{i\text{-}Pr}}$picolinate ligand, has been deposited in the CCSD as a personal communication: CCDC 194021; N. Nieger, C. Jung and E. Steckhan, 2002.
37 J. M. Stauber, A. L. Wadler, C. E. Moore, A. L. Rheingold and J. S. Figueroa, *Inorg. Chem.*, 2011, **50**, 7309–7316.
38 Y. Saito, J. Takemoto, B. Hutchinson and K. Nakamoto, *Inorg. Chem.*, 1972, **11**, 2003–2011.
39 M. Niemeyer and P. P. Power, *Angew. Chem., Int. Ed.*, 1998, **37**, 1277–1279.
40 R. J. Wright, M. Brynda and P. P. Power, *Inorg. Chem.*, 2005, **44**, 3368–3370.
41 L. Yang, D. R. Powell and R. P. Houser, *Dalton Trans.*, 2007, 955–964.
42 D. M. Jenkins, A. J. Di Bilio, M. J. Allen, T. A. Betley and J. C. Peters, *J. Am. Chem. Soc.*, 2002, **124**, 15336–15350.
43 D. M. Jenkins and J. C. Peters, *J. Am. Chem. Soc.*, 2005, **127**, 7148–7165.
44 $\mathrm{Cu(pic)_2}$: B. Zurowska, J. Ochocki, J. Mrozinski, Z. Ciunik and J. Reedijk, *Inorg. Chim. Acta*, 2004, **357**, 755–763.
45 $\mathrm{Cu(pic)_2}$: B. Zurowska, J. Mrozinski and Z. Ciunik, *Polyhedron*, 2007, **26**, 1251–1258.
46 $\mathrm{Cu(pic)_2{\cdot}H_2O}$: P. R. Faure, H. Loiseleur and G. Thomas-David, *Acta Crystallogr.*, 1973, **B29**, 1890–1893.
47 $\mathrm{Cu(pic)_2{\cdot}H_2O}$: P. Segl'a, M. Jamnicky, M. Koman;, J. Sima and T. Glowiak, *Polyhedron*, 1998, **17**, 4525–4533.
48 $\mathrm{Cu(pic)_2{\cdot}H_2O}$: M. Du, X.-H. Bu;, M. Shionoya and M. Shiro, *J. Mol. Struct.*, 2002, **607**, 155–161.
49 $\mathrm{Cu(pic)_2{\cdot}2H_2O}$: M. Mikuriya, H. Azuma, R. Nukada, Y. Sayama, K. Tanaka, J.-W. Lim and M. Handa, *Bull. Chem. Soc. Jpn.*, 2000, **73**, 2493–2498.
50 $\mathrm{Cu(pic)_2{\cdot}K[SCN]}$: F. S. Stephens, *J. Chem. Soc. A*, 1970, 2377–2379.
51 P. Comba, *Coord. Chem. Rev.*, 2000, **200–202**, 217–245.
52 M. Chatterjee, S. Ghosh and A. Kumar Nandib, *Polyhedron*, 1997, **16**, 2917–2923.
53 D. M. Stearns and W. H. Armstrong, *Inorg. Chem.*, 1992, **31**, 5178–5184.
54 B. N. Figgis, C. L. Ratson, R. P. Sharma and A. H. White, *Aust. J. Chem.*, 1978, **31**, 2545–2548.
55 C. Pelizzi and G. Pelizzi, *Transition Met. Chem.*, 1981, **6**, 315–316.
56 A. B. Pangborn, M. A. Giardello, R. H. Grubbs, R. K. Rosen and F. J. Timmers, *Organometallics*, 1996, **15**, 1518–1520.
57 W. L. F. Arnarego and C. L L. Chai, *Purification of Laboratory Chemicals*, Elsevier, 5th edn, 2003.
58 L. E. Manzer, *Inorg. Synth.*, 1982, **21**, 135–140.
59 M. C. Burla, R. Caliandro, M. Camalli, B. Carrozzini, G. L. Cascarano, L. De Caro, C. Gaicovazzo, G. Polidori and R. Spagna, *J. Appl. Crystallogr.*, 2005, **38**, 381–388.
60 G. M. Sheldrick, *Acta Crystallogr.*, 2008, **A64**, 112–122.